Rate and memory effects in bifurcation-induced tipping

Julia Cantisán,[1] Serhiy Yanchuk,[2,3] Jesús M. Seoane,[1]
Miguel A. F. Sanjuán,[1,4] and Jürgen Kurths[5,3]
[1]*Nonlinear Dynamics, Chaos and Complex Systems Group, Departamento de Física, Universidad Rey Juan Carlos Tulipán s/n, 28933 Móstoles, Madrid, Spain*
[2]*Department of Mathematics, Humboldt University Berlin, 12489 Berlin, Germany*
[3]*Potsdam Institute for Climate Impact Research, 14473 Potsdam, Germany*
[4]*Department of Applied Informatics, Kaunas University of Technology Studentu 50-415, Kaunas LT-51368, Lithuania*
[5]*Department of Physics, Humboldt University Berlin, 12489 Berlin, Germany*

(Received 10 March 2023; accepted 20 July 2023; published 3 August 2023)

A variation in the environment of a system, such as the temperature, the concentration of a chemical solution, or the appearance of a magnetic field, may lead to a drift in one of the parameters. If the parameter crosses a bifurcation point, the system can tip from one attractor to another (bifurcation-induced tipping). Typically, this stability exchange occurs at a parameter value beyond the bifurcation value. This is what we call, here, the shifted stability exchange. We perform a systematic study on how the shift is affected by the initial parameter value and its change rate. To that end, we present numerical simulations and partly analytical results for different types of bifurcations and different paradigmatic systems. We show that the nonautonomous dynamics can be split into two regimes. Depending on whether we exceed the numerical or experimental precision or not, the system may enter the nondeterministic or the deterministic regime. This is determined solely by the conditions of the drift. Finally, we deduce the scaling laws governing this phenomenon and we observe very similar behavior for different systems and different bifurcations in both regimes.

DOI: 10.1103/PhysRevE.108.024203

I. INTRODUCTION

The behavior of a dynamical system can be classified depending on the value of its parameters. Usually, this is represented by bifurcation diagrams, where the attractors are depicted for each region of parameters. For a fixed set of parameters and equations, the system remains in one of the corresponding attractors, for example, a fixed point, a limit cycle, a chaotic attractor, etc. However, in nature, this equilibrium is usually perturbed by the system's environment. Real-world systems are open and external perturbations can be modeled as a time variation of the parameters. A change in the parameters can cause the system to tip from one attractor to another, leading to a (sometimes drastic) regime shift. There are many examples of this sudden transition in different fields such as ecology [1] or climate dynamics [2]. Furthermore, this phenomenon may be desirable and one can then design an input that causes the system to tip. For instance, this is the case of experiments that involve transitions through critical temperatures and yield phase changes [3].

There are many different ways in which the variation of a parameter can lead to a regime shift. Following Ref. [4], they can be classified in three categories: noise-induced tipping (N-tipping), rate-induced tipping (R-tipping), and bifurcation-induced tipping (B-tipping). In the case of N-tipping, a parameter suffers fluctuations that force the system to abandon the attractor and tip to another one. For R-tipping [5], the rate at which a parameter drifts is sufficiently fast that the system fails to track the current attractor. Finally, B-tipping occurs when the parameter is slowly varying and crosses a bifurcation, forcing the system to tip. This tipping occurs because the attractor becomes a repeller past the bifurcation value.

Here, we deal with parameter drifts that lead to B-tipping, also called dynamic bifurcations [6,7] or slow passage through a bifurcation [8,9] in previous literature. This phenomenon has been studied from different perspectives, exploring concepts such as tipping probability in multistable systems, scenario-dependent basins, or early-warning indicators [10–15]. We focus on describing in a systematic way the process of tipping, specifically the shift phenomenon [16]. It has been observed that in systems with a parameter drift the tipping appears for a value of the parameter p different from the bifurcation value p_b. We call this value the critical value p_{cr}, which is $p_{\mathrm{cr}} > p_b$ (with increasing p). In systems with a faster parameter drift and a parameter-dependent attractor, R-tipping may appear for $p_{\mathrm{cr}} < p_b$. However, we restrain ourselves to the study of B-tipping. The shift phenomenon has also been referred to as the delay phenomenon, emphasizing the temporal delay in the tipping, $t_{\mathrm{cr}} > t_b$, rather than the shift in the parameter. Both terms are equivalent as the parameter depends on time. In Ref. [17], the time between p_{cr} and p_b is called borrowed time, to point out that in this time window the attractor no longer exists, although the system is still tracking an unstable object that appears at t_b, and it is still possible to avoid the tipping by reversing the drift.

The value of the shift $p_b - p_{\mathrm{cr}}$ is scenario dependent and it may vary with the parameter change rate ε. We call this the rate effect. This effect has been recently explored for complex systems such as maps with chaotic attractors [18,19], flows

 ©2023 American Physical Society

with chaotic attractors [20], and time-delayed systems [21]. Another interesting variable that can affect the value of $p_{\rm cr}$ is the initial value of the parameter p_0. This implies that the system has memory and that the distance to the bifurcation is relevant even in the case when the equilibrium that loses stability is parameter independent. The memory effect has been less studied in Refs. [8,22] and it usually does not take into account the rate effects and their interplay.

In this paper, we aim at a systematic study of the shift phenomenon that appears in B-tipping. We show that the system's dynamics is naturally split into two regimes: deterministic and nondeterministic, depending on whether noise plays an essential role or not. The nondeterministic case implies that the system's trajectory reaches the neighborhood of an attractor that is smaller than the threshold of the numerical noise. This is a typical situation occurring for a small change rate ε, as the local convergence to an attractor is exponential away from the bifurcation. Also, realistic systems are always subject to some level of noise, and experimental setups have a finite precision. In the deterministic regime, the noise threshold is not reached. This is usually related to faster drifts when the system has no time to relax and come closer to an attractor. We explore the rate and memory effects in the two regimes for different paradigmatic systems and different bifurcations. We obtain the analytical scaling laws that govern these processes and compare them with the numerical results.

The article is organized as follows. In Sec. II, we introduce the systems and bifurcations and the numerical techniques used to analyze them. In Sec. IV, we present the results for the deterministic regime, whereas in Sec. V we present the ones dealing with the nondeterministic regime. The rate and memory effects are explored in the two regimes, and both numerical and analytical calculations are presented. We provide concluding remarks at the end.

II. SYSTEMS AND BIFURCATIONS

We choose paradigmatic examples of dynamical systems with different types of bifurcations as our aim is to study common responses to a changing parameter that crosses a bifurcation. To that end, we proceed in the same way for every system and compare the behavior in each case. We choose one of the parameters and we make it evolve linearly with time at a small but non-negligible rate ε. Depending on the natural timescale of the system, we take ε in the range of 10^{-5}–10^{-2}. We change the parameter according to the following rule:

$$p(t) = \begin{cases} p_0 & \text{for } t < t_1 \\ p_0 + \varepsilon \cdot (t - t_1) & \text{for } t > t_1 \end{cases} \tag{1}$$

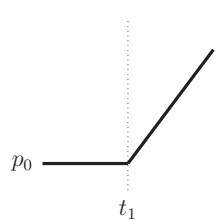

where t_1 is the time for which the parameter drift starts. In this way, we give the system some time to evolve before the shift in the parameter begins. At some point after t_1, the parameter crosses a bifurcation and the tipping is expected to be observed with some delay.

Specifically, we study the pitchfork and subcritical Hopf bifurcations in the Lorenz system, the supercritical Hopf bifurcation in the FitzHugh-Nagumo model, and the period-doubling bifurcation in the Rössler system. By analyzing these systems, we cover some common bifurcations, including the period-doubling, which can lead to chaos. The following ordinary differential equation solvers are used for the numerical integration: ode78 [Runge-Kutta 8(7)] and ode15s [variable-step, variable-order solver]. The latter method seems to capture the repulsion from an unstable attractor in a better way, but both of them yield quantitatively the same results.

A. Lorenz system

The Lorenz system [23] was proposed by Lorenz as a simple model of convection dynamics in the atmosphere (Rayleigh-Bénard convection). The equations read as follows:

$$\begin{aligned} \dot{x} &= -\sigma x + \sigma y, \\ \dot{y} &= rx - y - xz, \\ \dot{z} &= -\beta z + xy, \end{aligned} \tag{2}$$

where σ, β, and r are the system parameters. In the context of convection dynamics, σ is the Prandtl number and is characteristic of the fluid, β depends on the geometry of the container, and r is the Rayleigh number that accounts for the temperature gradient. In this context, x represents the rotation frequency of convection rolls, while y and z correspond to variables associated with the temperature field. We fix the classical parameter values of $\sigma = 10$ and $\beta = 8/3$, and we consider r as a time-dependent parameter $r(t)$, following Eq. (1).

In the frozen-in system, where r is a fixed parameter, we find successive bifurcations (see Ref. [20] for their brief description). Here, we focus on the pitchfork and subcritical Hopf bifurcations that occur at $r = 1$ and $r = 24.74$, respectively. The rate effect for the heteroclinic bifurcation was analyzed previously in Ref. [20]. In the pitchfork bifurcation, the fixed point in the origin loses stability and two other fixed points are created:

$$C^{\pm} = [\pm\sqrt{\beta(r-1)}, \pm\sqrt{\beta(r-1)}, r-1], \tag{3}$$

while in the subcritical Hopf bifurcation, $C^{\pm}$ lose stability and a chaotic attractor, born at $r = 24.06$, remains as the only attractor.

Turning to the time-dependent parameter scenario, the time series of a trajectory crossing these bifurcations can be seen in Figs. 1(a) and 1(b). The time at which the parameter r reaches the bifurcation and the critical value (t_b and $t_{\rm cr}$) are marked. We consider the condition for tipping to be a threshold of $\eta_{\rm cr} = 10^{-2}$ for the distance from the equilibrium (the origin in the case of the pitchfork bifurcation and $C^{\pm}$ in the case of the subcritical Hopf bifurcation). When the threshold is exceeded, the system is considered to change from one regime to another. In both cases, the system tips to another attractor some time after the equilibrium loses stability at t_b.

B. FitzHugh-Nagumo system

The FitzHugh-Nagumo (FHN) model [24,25] is a reduction of the four-dimensional Hodgkin-Huxley model [26] to a

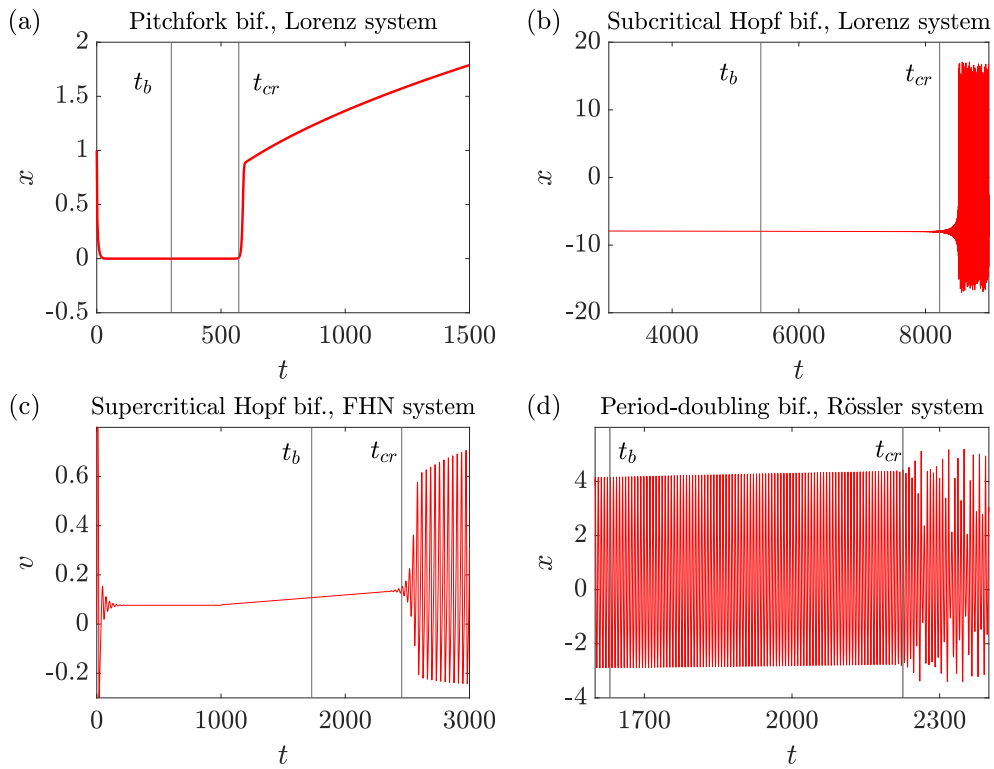

FIG. 1. Time series showing the bifurcation-induced tipping. The parameter drift starts at (a) $t_1 = 100$, (b) $t_1 = 1000$, (c) $t_1 = 1000$, and (d) $t_1 = 300$. It can be seen that the tipping does not occur at the bifurcation value t_b, rather it occurs at a posterior value of $t_{cr} > t_b$. Thus, we observe the shift phenomenon.

two-variable model. The latter was a very successful model of the initiation and propagation of neural action potential using a squid axon. The simplified version of the FitzHugh-Nagumo model reads

$$\begin{aligned} \dot{v} &= -v(v-a)(v-1) - w + I, \\ \dot{w} &= b(v - \gamma w), \end{aligned} \tag{4}$$

where the membrane potential v is the main observable, while w models a slow recovery current and I is the magnitude of the stimulus current. The constants a, b, and γ are kinetic parameters. We fix $a = 0.2$, $b = 0.05$, and $\gamma = 0.4$, and I is going to be the drifting variable, $I(t)$, following Eq. (1).

For the frozen-in version of this system, where I is a fixed parameter, we find a supercritical Hopf bifurcation at $I_b = 0.273$ [27]. For $I < I_b$, there is a fixed point $P^* = (v^*, w^*)$, which satisfies

$$-v^*(v^* - a)(v^* - 1) - v^*/\gamma + I = 0, \quad w^* = v^*/\gamma, \tag{5}$$

and depends on the value of I. A limit cycle appears for $I > I_b$.

If we let I vary with time at small but non-negligible rates and we cross I_b, we observe the transition from the equilibrium given by Eq. (5) to a periodic solution [see Fig. 1(c)]. We consider the threshold for the distance from the equilibrium P^* to be $\eta_{cr} = 10^{-2}$. Once this threshold is exceeded, the system is considered to have tipped. As can be seen, the tipping occurs at $t_{cr} > t_b$. This window of time is the borrowed time, in which the equilibrium has lost stability, but the system is still tracking it.

C. Rössler system

The last system we analyze was proposed by Rössler in 1976 [28] as a simple model for continuous chaos. The equations read

$$\begin{aligned} \dot{x} &= -y - z, \\ \dot{y} &= x + ay, \\ \dot{z} &= b + z(x - c), \end{aligned} \tag{6}$$

where a, b, and c are real parameters. In this case, we take a as the parameter that depends on time, $a(t)$, following Eq. (1) and we fix $b = 2$ and $c = 4$.

In the frozen-in version of Eq. (6), where a is fixed, the Rössler system exhibits a transition to chaos through a period-doubling bifurcation, similar to that of the logistic map. For our parameter values, the first transition is found at $a_b = 0.333$.

When we let a vary with time, we observe a transition like the one in Fig. 1(d). As can be seen, the periodical trajectory becomes chaotic after t_{cr}. The reason for this is that our change rate is too fast to observe all the doublings in between as they are too close. For instance, to observe the next transition at $a = 0.374$, the maximum rate is $\varepsilon = 10^{-5}$. For later transitions, the rate would decrease.

In this case, the tipping condition is the loss of periodicity. When the maxima of the time series do not appear periodically, the system is considered to have tipped to the chaotic attractor. To take into account that the period slightly increases for $t > t_1$ (as the period changes with the value of the parameter), we take a tolerance of 10^{-1} beyond which the trajectory is considered to have lost periodicity.

III. NONAUTONOMOUS DYNAMICS: DETERMINISTIC AND NONDETERMINISTIC REGIMES

When we let the parameters evolve with time at small but non-negligible rates in the previously presented systems, these systems become nonautonomous. Furthermore, the parameter $p(t)$ can be seen as a slow variable in contrast with the other variables that are said to be fast. As a result, our nonautonomous system presents a strong timescale separation. It is the interaction between the fast and slow variables of the system that causes the delayed or shifted tipping [29].

The nonautonomous dynamics presents two different scenarios depending on the characteristic of the drift. These are what we called the deterministic and nondeterministic regimes. Before the bifurcation value is reached, the trajectories approach the equilibrium x_0. If this phase is long enough, the trajectory may reach a distance from the equilibrium that may be smaller than the numerical accuracy or the noise level in an experiment. This can be achieved by setting a large value of t_1 and/or by setting a small value of ε. In both cases, the system has the time to approach the equilibrium exceeding the numerical or experimental precision. Beyond this threshold, noise plays a part and the maximum deviation of the distance from the equilibrium does not vary. This is the situation that occurs in the nondeterministic regime. On the contrary, if the threshold is not exceeded, we remain in the deterministic regime.

After the bifurcation value p_b is reached, the equilibrium loses stability, but the tipping is not observed until a larger value of the parameter ($p_{\rm cr} > p_b$) due to the timescale separation. We show that the tipping phenomenon has different characteristics in each regime.

A more complex situation is that in which the equilibrium x_0 depends on the parameter too. This makes it more difficult for the system to track the equilibrium once the drift starts. That is the case of the subcritical and supercritical Hopf bifurcations and the period-doubling bifurcation presented before. In this situation, the nondeterministic regime requires smaller values of ε to be able to approach the equilibrium past the threshold. Also, increasing t_1 is no longer beneficial to entering the nondeterministic regime.

In the following sections, we let the parameters evolve with time for each regime and we study the shift phenomenon using the described tipping conditions. We describe both numerically and partly analytically the memory effect (dependence of $p_{\rm cr}$ on p_0) and the rate effect (dependence of $p_{\rm cr}$ on ε).

IV. DETERMINISTIC REGIME

An autonomous dynamical system with constant parameters converges to an attractor after some transient time. However, if the external conditions change, and one of the parameters changes with time, we may observe a stability exchange as the system tips from one attractor to another.

In this section, we analyze the phenomenon of shifted stability exchange in the deterministic regime, that is, when the precision threshold is not reached and noise does not affect the system's behavior. We analyze the memory and the rate effect in this scenario and we approach this question from two sides: analytical and numerical.

A. Shifted stability exchange: Analytical approach

We aim to obtain an expression for the shift phenomenon that enables us to calculate the critical value of the parameter $p_{\rm cr}$. Analytically, we deal with the simplest case of a fixed point that loses stability due to the crossing of a bifurcation. We start with the system

$$\dot{x} = f[x; p(t)], \tag{7}$$

with a parameter-independent equilibrium, which we set to zero without loss of generality: $f(0; p) = 0$. The parameter p changes with time according to Eq. (1), that is: $\dot{p} = \varepsilon\mathcal{P}(t)$, where $\mathcal{P}(t)$ is the Heaviside function $\mathcal{P}(t) = H(t - t_1)$.

This nonautonomous system possesses an invariant set (slow manifold), $x = 0$. The linear stability of the set $x = 0$ is governed by the linearization

$$\begin{aligned} \dot{\xi} &= Df(0; p)\xi, \\ \dot{p} &= \varepsilon\mathcal{P}(t), \end{aligned} \tag{8}$$

where $Df(0; p) = \frac{\partial}{\partial x} f(0; p)$. Here, we use the property $\frac{\partial}{\partial p} f(0; p) = 0$. Now, we assume that this linearized system has one leading (critical) eigendirection with the eigenvector $v(p)$ and the eigenvalue $\lambda(p)$ so that

$$Df(0; p)v(p) = \lambda(p)v(p),$$

where $\lambda(p_b) = 0$ and $\lambda(p) < 0$ for $p < p_b$, and $\lambda(p) > 0$ for $p > p_b$.

This assumption holds true close to a generic pitchfork or transcritical bifurcation. Thus, from the systems presented above, these calculations are valid only for the pitchfork bifurcation in the Lorenz system. Despite this limitation, the numerical approach will show that the system's response is very similar for more complex bifurcations. We also consider the case that all other eigendirections are stable, and we can restrict Eq. (8) to the critical direction, leading to the following system:

$$\begin{aligned} \dot{\eta} &= \lambda(p)\eta, \\ \dot{p} &= \varepsilon\mathcal{P}(t), \end{aligned} \tag{9}$$

where η measures the Euclidian distance from the equilibrium.

Notice that we consider the case where the equilibrium x_0 does not depend on the parameter p. Otherwise, the simple approach above needs to be modified [29–32]. In the case of parameter-dependent equilibrium, not only B-tipping but also R-tipping is possible. In this case, for certain rates, the tipping can occur before, not after, the bifurcation value.

Since the parameter p is a function of time following Eq. (1), during the time interval $t \in [0, t_1]$, the parameter is

constant and the equation for $\dot{\eta}$ has a constant coefficient $\lambda(p_0)$. Hence,

$$\eta(t_1) = \eta_0 e^{\lambda(p_0)t_1}, \tag{10}$$

where $\eta(0) = \eta_0$. Further, for $t \geqslant t_1$, the distance from the equilibrium changes as

$$\dot{\eta} = \lambda[p_0 + \varepsilon(t - t_1)]\eta, \tag{11}$$

which can be solved as follows:

$$\eta(t) = \eta(t_1)\exp\left\{\int_{t_1}^{t} \lambda[p_0 + \varepsilon(t - t_1)]dt\right\} \tag{12}$$

or, equivalently

$$\begin{aligned}\eta(t) &= \eta(t_1)\exp\left\{\frac{1}{\varepsilon}\int_{p_0}^{p_0+\varepsilon(t-t_1)} \lambda(p)dp\right\}\\ &= \eta_0 \exp\left\{\lambda(p_0)t_1 + \frac{1}{\varepsilon}\int_{p_0}^{p_0+\varepsilon(t-t_1)} \lambda(p)dp\right\}.\end{aligned} \tag{13}$$

As previously mentioned, we take the condition for the escape from the equilibrium to be

$$\eta_{\rm cr} = \eta(t_{\rm cr}), \tag{14}$$

where $\eta_{\rm cr}$ is a small threshold, after which the system is considered to be away from the equilibrium, and $t_{\rm cr}$ is the escape time. Using Eqs. (13) and (14), we obtain

$$\lambda(p_0)t_1 + \frac{1}{\varepsilon}\int_{p_0}^{p_{\rm cr}} \lambda(p)dp = \ln\frac{\eta_{\rm cr}}{\eta_0}, \tag{15}$$

where $p_{\rm cr} = p_0 + \varepsilon(t_{\rm cr} - t_1)$. Denoting the constant

$$C := \ln\frac{\eta_{\rm cr}}{\eta_0}, \tag{16}$$

we obtain the following condition for determining the critical parameter value $p_{\rm cr}$:

$$\int_{p_0}^{p_{\rm cr}} \lambda(p)dp = \varepsilon[C - \lambda(p_0)t_1]. \tag{17}$$

As can be seen, the value of the shift $(p_{\rm cr} - p_b)$ depends on the initial value of the parameter p_0 leading to a memory effect. Furthermore, it depends on the change rate ε; this is, the rate effect is present as well.

As an example, we compute Eq. (17) for the pitchfork bifurcation in the Lorenz system. Now our parameter p is the Rayleigh number r. The eigenvalues for the equilibrium at the origin are

$$\begin{aligned}\lambda_1 &= -\beta,\\ \lambda_{2,3} &= \tfrac{1}{2}(-1 - \sigma \pm \sqrt{4r\sigma + \sigma^2 - 2\sigma + 1}).\end{aligned}$$

For $r < 1$, all the eigenvalues are negative. At $r = 1$, λ_2 changes sign, so the equilibrium at the origin becomes unstable giving rise to the pitchfork bifurcation. Thus, $r_b = 1$ and the critical eigenvalue in this case is $\lambda_2 =: \lambda$. For our parameter values, it reads

$$\lambda = \tfrac{1}{2}(-11 + \sqrt{81 + 40r}). \tag{18}$$

Now, integrating the eigenvalue as in Eq. (17), we get

$$\begin{aligned}&\frac{1}{2}\int_{r_0}^{r_{\rm cr}} \left(-11 + \sqrt{81 + 40r}\right)dr\\ &\quad= \frac{-11(r_{\rm cr} - r_0)}{2}\\ &\qquad+ \frac{1}{120}[(40r_{\rm cr} + 81)^{3/2} - (40r_0 + 81)^{3/2}].\end{aligned} \tag{19}$$

As we are interested in representing $r_1 = r_{\rm cr} - r_b$ against $r_2 = r_b - r_0$, that is, the distances before and after the bifurcation, we apply a change of variables so that $r_{\rm cr} = r_1 + r_b$ and $r_0 = r_b - r_2$. Finally, using Eq. (17), we obtain

$$\begin{aligned}&\frac{-11(r_1 + r_2)}{2} + \frac{1}{120}\{[40(r_1 + r_b) + 81]^{3/2}\\ &\qquad - [40(r_b - r_2) + 81]^{3/2}\}\\ &\quad= \varepsilon\left[C - \frac{-11\sqrt{81 + 40(r_b - r_2)}}{2}t_1\right].\end{aligned} \tag{20}$$

To obtain the value of C, we take the initial distance to the equilibrium $\eta_0 = 1$ and the critical distance $\eta_{\rm cr} = 10^{-2}$, following the criterion presented in Sec. II. We also fix the time at which the parameter starts drifting to $t_1 = 100$. Equation (20) can be numerically solved to obtain the curves in Fig. 2(a) for different values of ε.

The memory effect is clear in the figure: for initial values of the parameter closer to the bifurcation value, the tipping occurs before. This relation is not linear in general. It is linear only for the case of simple systems in which the eigenvalue λ is linearly dependent on the parameter: $\lambda(p) = mp$, where $m \in \mathbb{R}$. This is not the case for the Lorenz system [see Eq. (18)]. The linearization of the eigenvalue was considered in Ref. [27] taking a small value of ε, but here we obtain the general expression.

The rate effect can also be seen in Fig. 2(a): for a fixed value of r_0, the shift increases with the change rate.

B. Shifted stability exchange: Numerical approach

Now, we analyze the shifted stability exchange numerically. However, we restrain to the case that the numerical threshold is not reached and the dynamics are deterministic. We integrate Eqs. (2), (4), and (6) with the parameter drift starting at (a) $t_1 = 100$, (b) $t_1 = 1000$, (c) $t_1 = 1000$, and (d) $t_1 = 300$, for different rates ε. These values are chosen to skip the transient behavior before the drift starts. We show the shift phenomenon for all the bifurcations in Fig. 2. The values of ε and p_0 are also different from one system to another, attending to the natural timescale and the presence of other bifurcations that limit the maximum value of $p_{\rm cr} - p_0$.

Comparing the analytical and numerical data for the pitchfork bifurcation, it can be seen that both approaches match for a certain region, but afterwards the numerical data yield a plateau. This plateau, present in all the other bifurcations too, corresponds to the nondeterministic regime. In that regime, the system has time enough to relax and approach the attractor beyond the numerical precision. This can be the case for slow enough rates or values of r_0 far enough from the bifurcation. In these cases, the numerical noise plays the role of a

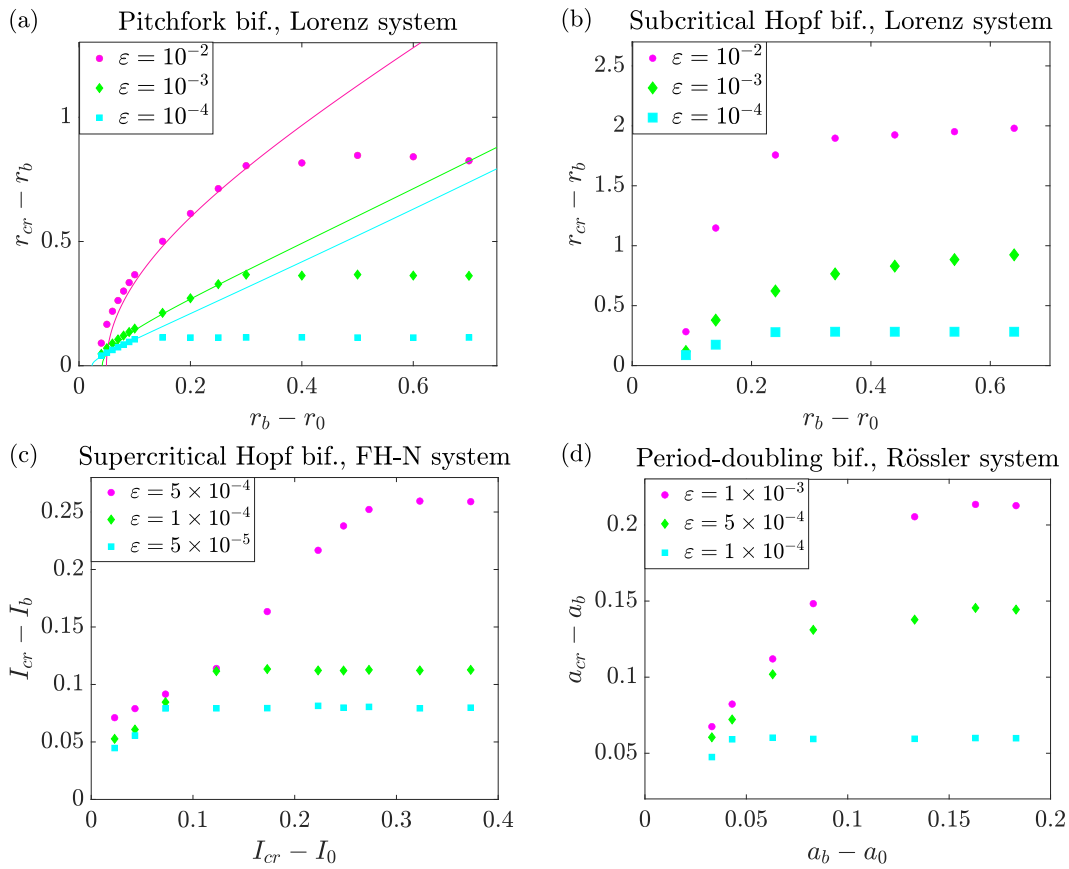

FIG. 2. Memory and rate effects for different bifurcations and systems in the deterministic regime. The curves in panel (a) are analytically calculated, while the points in panels (a), (b), (c), and (d) are numerically calculated. The difference in both approaches comes from the impact of the numerical noise that causes the memory loss as we enter the nondeterministic regime. This can be seen in the form of plateaus. Before that, in the deterministic regime, both approaches can be seen to match for the pitchfork bifurcation.

memory-loss agent. We explore the nondeterministic regime in more detail in the following section.

Notice that in the deterministic regime all the systems' responses are quite similar to what was predicted by Eq. (17). The analytical calculation is valid for a system that has one leading (critical) eigendirection and for equilibria that do not depend on the parameter, which holds for such bifurcations as the pitchfork. However, we can see that even for more complex bifurcations such as the period-doubling, we obtain a similar memory effect. In all cases, the shift increases with ε and also increases with the initial distance to the bifurcation before entering the nondeterministic regime.

Another parameter that may seemingly affect the shift phenomenon is t_1. It plays a role similar to that of ε. For small values of t_1, the system has no time to relax before the parameter drift starts, while for large t_1, we enter again the nondeterministic regime and we observe a memory loss. This can be seen in Fig. 3 for the pitchfork bifurcation and $\varepsilon = 10^{-2}$. In Fig. 3(a), we observe how the memory loss appears even for small values of t_1 when the initial value of the parameter is far enough from the bifurcation, allowing the system to relax once again. On the right side, we can see how the different trajectories approach the equilibrium at the origin for $r_0 = 0.9$; that is, $r_b - r_0 = 0.1$. Notice the different orders of magnitude in the y axis and the presence of numerical noise for the largest value of t_1. For $t_1 = 50$ and 200, the trajectory is deterministic, while for $t_1 = 1000$, we enter the nondeterministic regime.

For the other bifurcations, changing t_1 barely affects the shift as the value of the equilibrium also depends on the value of the parameter [see Eq. (3) or (5)]. Note that, on the contrary, for the pitchfork bifurcation the equilibrium is fixed at the origin for $r < r_b$. This implies that for the other bifurcations it is more difficult to track the equilibrium for $t_1 < t < t_b$. Thus, in those cases getting closer to the equilibrium before the parameter drift starts is not enough to observe the memory loss. Only reducing the value of ε can maintain the system in the nondeterministic regime.

Finally, for the case that the equilibrium depends on the drifting parameter $x_0(p)$, it has been reported that in Hopf bifurcations the shift does not depend on ε if ε is kept sufficiently small [8,27]. This can be seen in Fig. 2(c) for the FHN system as long as we are sufficiently close to the bifurcation. The pink, green, and blue points come very close and the shift can be said to be independent of ε in the first approximation.

V. NONDETERMINISTIC REGIME

In this section we explore the shifted stability exchange when the system enters the nondeterministic regime. This

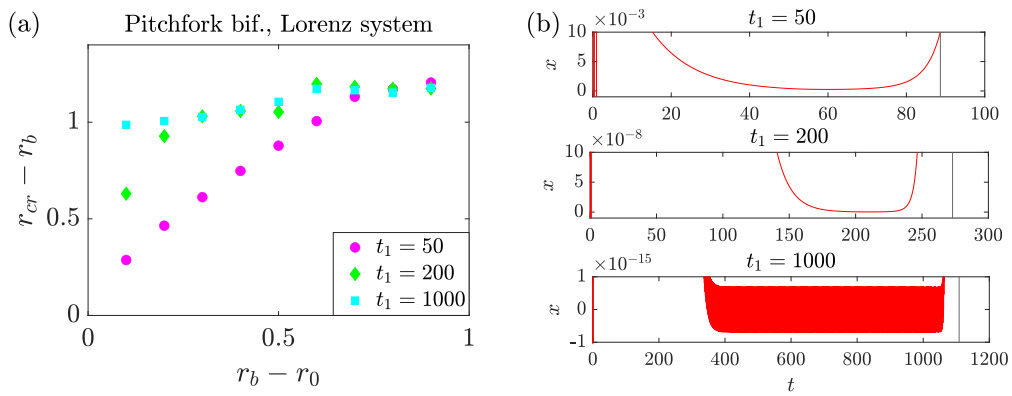

FIG. 3. Memory effect for different values of t_1. In panel (a), it can be seen that the shift is less pronounced for small values of t_1. For values of r_0 far enough from the bifurcation, this effect disappears ($r_{\rm cr}$ becomes independent of t_1) as the three trajectories enter the nondeterministic region. In panel (b), we show the time series for $r_0 = 0.9$, that is, $r_b - r_0 = 0.1$. The vertical black lines correspond to $t = t_{\rm cr}$. Notice that, for $t_1 = 1000$, numerical noise is already present and causes the memory loss.

means that the system reaches the precision threshold and noise affects the dynamics, causing a memory loss. We present analytical and numerical results for the systems presented in Sec. II as well.

A. Shifted stability exchange: Analytical approach

We aim to obtain an analytical expression for $p_{\rm cr}$ that takes into account that the system reaches a threshold $\eta_n = \eta(t_n)$ of the numerical precision within the observable time interval $t_n < t_{\rm cr}$. Depending on whether the threshold is reached before or after the drift starts, we can classify the system's behavior in two cases, A and B.

(A) The system reaches the numerical precision threshold before the parameter drift starts ($t_1 > t_n$). In this case, the dynamics of the system can be divided into the following steps:

(i) exponential convergence to the equilibrium with the fixed rate $\lambda(p_0)$ until t_n;

(ii) drifting phase within the numerical precision error for $t \in [t_n, t_b]$, $t_b > t_1$; and

(iii) nonautonomous deterministic dynamics according to Eq. (11) on $[t_b, t_{\rm cr}]$, until the escape threshold $\eta_{\rm cr} = \eta(t_{\rm cr})$ is reached.

(B) The threshold is not reached before the parameter drift starts ($t_1 < t_n$). In this case, the dynamics is divided into the following steps:

(i) exponential convergence to the equilibrium with the fixed rate $\lambda(p_0)$ until t_1;

(ii) nonautonomous deterministic dynamics according to Eq. (11) on $[t_1, t_n]$, until the numerical precision threshold $\eta_n = \eta(t_n)$ is reached;

(iii) drifting phase within the numerical precision error for $t \in [t_n, t_b]$, $t_b > t_1$; and

(iv) nonautonomous deterministic dynamics according to Eq. (11) on $[t_b, t_{\rm cr}]$, until the escape threshold $\eta_{\rm cr} = \eta(t_{\rm cr})$ is reached.

In both cases, the system starts feeling the repulsion at the bifurcation value, that is, when the equilibrium loses stability. From this moment, the dynamics becomes deterministic again.

Starting from the reduced equation for the distance from the equilibrium, Eq. (11), and taking into account Eqs. (10)–(13), we obtain the following expressions for the distance $\eta(t)$ for case A:

(A-i)

$$\eta_n = \eta_0 e^{\lambda(p_0)t_n}, \tag{21}$$

(A-ii)

$$\eta(t_b) = \eta_b = \eta_n = \eta_0 e^{\lambda(p_0)t_n}, \tag{22}$$

(A-iii)

$$\eta(t) = \eta(t_b)\exp\left\{\int_{t_b}^{t} \lambda[p_0 + \varepsilon(t - t_1)]dt\right\}. \tag{23}$$

During phase (A-ii), the maximum deviation does not vary, and there are fast fluctuations related to the numerical noise and particularities of the numerical integration scheme. We neglect these fluctuations and only take into account that the distance starts to grow exponentially after this phase from η_b. Equivalently, the integral in Eq. (23) can be written in terms of the parameter instead of time, leading to

$$\begin{aligned}\eta(t) &= \eta(t_b)\exp\left\{\frac{1}{\varepsilon}\int_{p_0+\varepsilon(t_b-t_1)}^{p_0+\varepsilon(t-t_1)} \lambda(p)dp\right\}\\ &= \eta_n \exp\left\{\frac{1}{\varepsilon}\int_{p_p}^{p_{\rm cr}} \lambda(p)dp\right\},\end{aligned} \tag{24}$$

with $p_{\rm cr} = p_0 + \varepsilon(t_{\rm cr} - t_1)$ and $p_b = p_0 + \varepsilon(t_b - t_1) \geqslant p_0$. Now, for $t = t_{\rm cr}$, we apply the escape condition so that we obtain

$$\int_{p_b}^{p_{\rm cr}} \lambda(p)dp = \varepsilon \ln \frac{\eta_{\rm cr}}{\eta_n}. \tag{25}$$

From this expression we can obtain the value of $p_{\rm cr}$, which does not depend on p_0. Thus, we observe a memory loss due to the presence of noise. This was already observed in Fig. 2 for the numerically calculated points: when the system entered the nondeterministic regime the points reached a plateau, indicating that the exchange of stability is independent of p_0.

On the other hand, Eq. (25) does depend on the change rate. Integrating this equation for the pitchfork bifurcation in

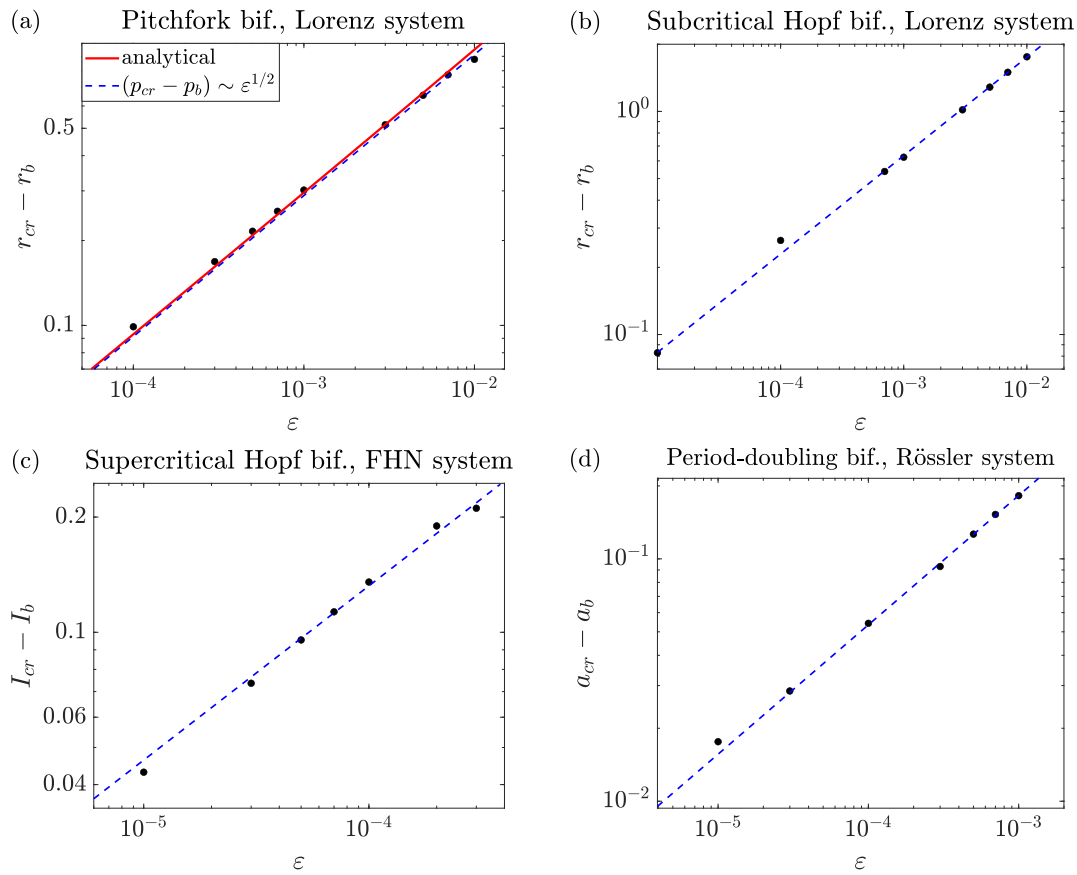

FIG. 4. Rate effect on the shifted stability exchange for different bifurcations and systems. The plots are in logarithmic scale for a better visualization. The red curve in panel (a) is analytically calculated from Eq. (25) and the points in panels (a), (b), (c), and (d) are numerically calculated. The response is similar in all systems: for higher change rates, the shift is larger and it seems to follow approximately the power law $(p_{\rm cr} - p_b) \sim \varepsilon^{1/2}$ in all cases (dashed blue lines).

the Lorenz system and considering $\eta_n = 10^{-19}$, we depict this dependence in Fig. 4(a) as a red curve. It is represented in logarithmic scale for a better visualization. This corresponds to representing the different heights of the plateaus from Fig. 2. We observe that the shift increases with increasing change rate.

Another clear implication of Eq. (25) is that $p_{\rm cr} \to p_b$ as $\varepsilon \to 0$. This implies that, as the shift tends to zero, we recover the frozen-in bifurcation diagram. This would be the case of a quasistatic parameter variation. Furthermore, for sufficiently small ε, the linearization $\lambda(p) \approx \lambda_0'(p - p_b)$ can be used, leading to

$$p_{\rm cr} = p_b + \sqrt{\frac{2\varepsilon}{\lambda_0'} \ln \frac{\eta_{\rm cr}}{\eta_n}},$$

which implies the square root scaling $(p_{\rm cr} - p_b) \sim \varepsilon^{1/2}$. This power law has been drawn in Fig. 4 as dashed blue lines for all the bifurcations. For the pitchfork bifurcation it is very similar to the red curve calculated using Eq. (25). And for the rest of the bifurcations, the numerically calculated points seem to match this approximation too. All in all, we find similar qualitative behavior for different bifurcations and systems following the power law $(p_{\rm cr} - p_b) \sim \varepsilon^{1/2}$.

For case B, we obtain analogously the following expression for the phase (B-iv):

$$\eta_b = \eta(t_b) = \eta_n, \tag{26}$$

and

$$\eta_{\rm cr} = \eta_n \exp\left\{\frac{1}{\varepsilon}\int_{p_b}^{p_{\rm cr}} \lambda(p)dp\right\}, \tag{27}$$

leading to the same expression, Eq. (25), for the escape as in case A. In case B, we find again that the memory is lost as in case A.

B. Shifted stability exchange: Numerical approach

Now, we numerically calculate $p_b - p_{\rm cr}$ for the nondeterministic regime. The values of t_1 remain the same as in the previous section and we fix p_0 to the following values: (a) $r_0 = 0.5$, (b) $r_0 = 24.5$, (c) $I_0 = 0.05$, and (d) $a_0 = 0.2$, which belong to the beginning of the plateaus in Fig. 2, and thus we make sure that we are in the nondeterministic regime. For these values, in all cases we find that $t_1 < t_n$, which is case A from Sec. V A.

As previously mentioned, we find a memory loss in this regime, which can be seen in the form of plateaus in Fig. 2. It was already suggested by Baer *et al.* [8] that adding a

TABLE I. Summary of the memory (p_{cr} dependence on p_0) and rate (p_{cr} dependence on ε) effects for the deterministic and nondeterministic regimes.

Deterministic regime	Nondeterministic regime
Memory effect	No memory effect
Rate effect	Rate effect: $(p_{cr} - p_b) \sim \varepsilon^{1/2}$

white Gaussian noise may destroy memory effects. However, we want to clarify here that we did not introduce noise in our equations. Instead, noise has arisen naturally from the precision restrictions of the numerical algorithms.

Regarding the rate effect, we present the results in Fig. 4. The points are depicted in logarithmic scale for a better visualization. As stated in the previous section, these numerically calculated points match the power law $(p_{cr} - p_b) \sim \varepsilon^{1/2}$ (dashed blue lines). This implies that, no matter the bifurcation or the system, we observe a similar response to a variation in the change rate.

These results are in agreement with previous work dealing with complex bifurcations such as the heteroclinic bifurcation in the Lorenz system [20] and the boundary crisis in the Duffing oscillator with delay [21]. In both cases, chaotic attractors that lose stability are involved; thus, they are not expected to follow our analytical calculations (the exponent in the power law differs from 1/2). However, qualitatively they present similar rate effects.

In Table I we summarize the different effects depending on the regime in which the system is found. For the deterministic regime, the shift depends on the initial value of the parameter p_0 and on ε. In particular, we observe that as $|p_b - p_0| \to 0$, the dependence on ε is less pronounced. On the other hand, for the nondeterministic regime memory loss occurs. Thus, the shift is independent of p_0 and we can approximate the shift as $(p_{cr} - p_b) \sim \varepsilon^{1/2}$.

VI. CONCLUSIONS AND DISCUSSION

We have studied the shifted stability exchange that occurs when a drifting parameter crosses a bifurcation point. This phenomenon causes that the tipping from one attractor to another appears for a parameter value beyond the bifurcation point. To this end, we have analyzed some paradigmatic systems to find common features of this phenomenon. We found that there are two regimes: deterministic and nondeterministic. For certain drift scenarios, when the rate of change of the parameter is sufficiently low, the system comes very close to an attractor so that the precision (numerical noise) does not allow it to be attracted any further. In this case, noise plays an important role and leads to the nondeterministic regime. This is a very common scenario as all numerical algorithms are subject to precision limits. Furthermore, this is also the regime of an experimental setup that has precision limits when approaching the attractor.

For the deterministic regime, we have derived the expression for the shift phenomenon, i.e., the value of p_{cr}, which depends on the initial value of the parameter (memory effect) and on the change rate (rate effect). In this case, the rate effect is more intense for initial values of the parameter further from the bifurcation. This expression is valid for bifurcations such as the pitchfork bifurcation, but the numerical calculations show similar qualitative behavior for more complex bifurcations such as the period-doubling bifurcation.

For the nondeterministic regime, we have observed that the noise acts as a memory-loss agent no matter if the threshold is reached before or after the drifting has started. We have derived the analytical expression for the shift and proved that it matches the numerical calculations too. For the rate effect, the system obeys a power law scaling of the type $(p_{cr} - p_b) \sim \varepsilon^{1/2}$ for all the systems and bifurcations. This implies that, if $\varepsilon \to 0$, then $p_{cr} \to p_b$, thus recovering the frozen-in bifurcation diagram.

Finally, we address the implications of our work. There is a lot of research that aims to predict when a system is going to tip [2,30,33,34], ending the so-called borrowed time between the bifurcation and the tipping. Sometimes this transition is undesirable as it might be the case of population extinction in the context of ecology or climate change due to anthropogenic causes. In other situations, the tipping might be desirable, but the shift should be minimized as much as possible. This is the case of some physical experiments, such as transitions through critical temperatures, in which the sweep in a parameter is costly. To this end, we consider that it is important to take into account the memory and rate effects described here.

ACKNOWLEDGMENTS

This work has been supported by the Spanish State Research Agency (AEI) and the European Regional Development Fund (ERDF, EU) under Project No. PID2019-105554GB-I00 (MCIN/AEI/10.13039/501100011033). The work of S.Y. was supported by the German Research Foundation DFG under Project No. 411803875.

[1] A. Hastings, K. C. Abbott, K. Cuddington, T. Francis, G. Gellner, Y. C. Lai, A. Morozov, S. Petrovskii, K. Scranton, and M. L. Zeeman, Transient phenomena in ecology, Science **361**, eaat6412 (2018).

[2] T. M. Lenton, H. Held, E. Kriegler, J. W. Hall, W. Lucht, S. Rahmstorf, and H. J. Schellnhuber, Tipping elements in the Earth's climate system, Proc. Natl. Acad. Sci. USA **105**, 1786 (2008).

[3] A. Majumdar, J. Ockendon, P. Howell, and E. Surovyatkina, Transitions through critical temperatures in nematic liquid crystals, Phys. Rev. E **88**, 022501 (2013).

[4] P. Ashwin, S. Wieczorek, R. Vitolo, and P. Cox, Tipping points in open systems: Bifurcation, noise-induced and rate-dependent examples in the climate system, Philos Trans. R. Soc. A **370**, 1166 (2012).

[5] S. Wieczorek, P. Ashwin, C. M. Luke, and P. M. Cox, Excitability in ramped systems: The compost-bomb instability, Proc. R. Soc. Ser. A **467**, 1243 (2011).

[6] C. Lobry, Dynamic bifurcations, in *Lecture Notes Mathematics* (Springer, Berlin, 1991), Vol. 1493, pp. 1–13.

[7] C. Baesens, Slow sweep through a period-doubling cascade: Delayed bifurcations and renormalisation, Phys. D: Nonlin. Phenom. **53**, 319 (1991).

[8] S. M. Baer, T. Erneux, and J. Rinzel, The slow passage through a Hopf bifurcation: Delay, memory effects and resonance, SIAM J. Appl. Math. **49**, 55 (1989).

[9] J. Penalva, M. Desroches, A. E. Teruel, and C. Vich, Slow passage through a Hopf-like bifurcation in piecewise linear systems: Application to elliptic bursting, Chaos **32**, 123109 (2022).

[10] A. Neishtadt, On stability loss delay for dynamical bifurcations, Discret. Contin. Dyn. Syst. Ser. S **2**, 897 (2009).

[11] B. Kaszás, U. Feudel, and T. Tél, Tipping phenomena in typical dynamical systems subjected to parameter drift, Sci. Rep. **9**, 8654 (2019).

[12] P. Ashwin, C. Perryman, and S. Wieczorek, Parameter shifts for nonautonomous systems in low dimension: Bifurcation- and rate-induced tipping, Nonlinearity **30**, 2185 (2017).

[13] Y. Song, W. Xu, and Y. Jiao, Bifurcation- and noise-induced tipping in two-parametric gene transcriptional regulatory system, Eur. Phys. J. Plus **137**, 68 (2021).

[14] N. Berglund and H. Kunz, Memory effects and scaling laws in slowly driven systems, J. Phys. A: Math. Gen. **32**, 15 (1999).

[15] N. Berglund and B. Gentz, Metastability in simple climate models: Pathwise analysis of slowly driven Langevin equations, Stochast. Dyn. **02**, 327 (2002).

[16] A. Neishtadt, Persistence of stability loss for dynamical bifurcations, I, Differ. Equations **23**, 1385 (1987).

[17] T. P. Hughes, C. Linares, V. Dakos, I. A. van de Leemput, and E. H. van Nes, Living dangerously on borrowed time during slow, unrecognized regime shifts, Trends Ecol. Evol. **28**, 149 (2013).

[18] O. V. Maslennikov and V. I. Nekorkin, Dynamic boundary crisis in the Lorenz-type map, Chaos **23**, 023129 (2013).

[19] O. V. Maslennikov, V. I. Nekorkin, and J. Kurths, Transient chaos in the Lorenz-type map with periodic forcing, Chaos **28**, 033107 (2018).

[20] J. Cantisán, J. M. Seoane, and M. A. F. Sanjuán, Transient dynamics of the Lorenz system with a parameter drift, Int. J. Bifurcation Chaos **31**, 2150029 (2021).

[21] J. Cantisán, J. M. Seoane, and M. A. F. Sanjuán, Transient chaos in time-delayed systems subjected to parameter drift, J. Phys.: Complexity **2**, 025001 (2021).

[22] J. Su, The phenomenon of delayed bifurcation and its analyses, in *Multiple-Time-Scale Dynamical Systems*, edited by C. K. R. T. Jones and A. I. Khibnik (Springer, New York, 2001), pp. 203–214.

[23] E. N. Lorenz, Deterministic nonperiodic flow, J. Atmos. Sci. **20**, 130 (1963).

[24] R. FitzHugh, Impulses and physiological states in theoretical models of nerve membrane, Biophys. J. **1**, 445 (1961).

[25] J. Nagumo, S. Arimoto, and S. Yoshizawa, An active pulse transmission line simulating nerve axon, Proc. IRE **50**, 2061 (1962).

[26] A. L. Hodgkin and A. F. Huxley, A quantitative description of membrane current and its application to conduction and excitation in nerve, J. Physiol. **117**, 500 (1952).

[27] S. M. Baer and E. M. Gaekel, Slow acceleration and deacceleration through a Hopf bifurcation: Power ramps, target nucleation, and elliptic bursting, Phys. Rev. E **78**, 036205 (2008).

[28] O. E. Rössler, An equation for continuous chaos, Phys. Lett. A **57**, 397 (1976).

[29] C. Kuehn, in *Multiple Time Scale Dynamics*, 1st ed., Applied Mathematical Sciences Vol. 191 (Springer, Cham, 2015), pp. 359–396.

[30] P. E. O'Keeffe and S. Wieczorek, Tipping phenomena and points of no return in ecosystems: Beyond classical bifurcations, SIAM J. Appl. Dyn. Syst. **19**, 2371 (2020).

[31] P. Ritchie, H. Alkhayuon, P. Cox, and S. Wieczorek, Rate-induced tipping in natural and human systems, EFUsphere, 10.5194/egusphere-2022-1176.

[32] P. D. Ritchie, J. J. Clarke, P. M. Cox, and C. Huntingford, Overshooting tipping-point thresholds in a changing climate, Nature (London) **592**, 517 (2021).

[33] J. C. Moore, Predicting tipping points in complex environmental systems, Proc. Natl. Acad. Sci. USA **115**, 635 (2018).

[34] S. K. Kim, H. J. Kim, H. A. Dijkstra, and S. I. An, Slow and soft passage through tipping point of the Atlantic Meridional Overturning Circulation in a changing climate, npj Clim. Atmos. Sci. **5**, 1 (2022).